Fine Structure of Thresholds in a Micromaser Pumped with Atom Clusters

G. M. D'Ariano, N. Sterpi, and A. Zucchetti

Dipartimento di Fisica "A. Volta," Università degli Studi di Pavia, via Bassi 6, I-27100 Pavia, Italy

(Received 13 June 1994)

We present the first quantum microscopic study of a micromaser with many atoms in the cavity. Excited atoms are injected in clusters with average number $\overline{N}$ up to 100. The stationary state of radiation is evaluated by means of a novel Green-function Monte Carlo technique. For $\overline{N} < N_{\rm ex}$ ($N_{\rm ex}$ being the number of excited atoms entering the cavity in a photon lifetime) the system behaves similarly to the one-atom maser. At $\overline{N} \simeq N_{\rm ex}$ a transition occurs to a novel cluster behavior, where a fine structure of thresholds emerges.

PACS numbers: 42.50.Dv, 42.50.Ar, 42.52.+x

In recent years the micromaser [1,2] has been extensively studied both experimentally and theoretically. Attention has been focused on the high-Q cavity one-atom maser, with interest devoted to fundamental issues related to the quantum mechanics of radiation in interaction with single atoms [3]. In this context the one-atom maser represents a fortunate situation, because analytical methods can be used [4] and the system can be realized experimentally [1]. Recently, theoretical descriptions of masers with few atoms simultaneously in the cavity have been faced—however, for no more than two atoms [5–7]. There, apart from the disappearance of trapping states [5,6], the main features of radiation remain similar to those of the one-atom case, whereas at the semiclassical level there are indications of new cooperative chaotic phenomena [7].

The availability of novel Monte Carlo techniques for simulating the master equation [8,9] now allows the study of the micromaser also for quite large numbers of atoms in the cavity, in a physical situation approaching the ordinary macroscopic maser. With the aim of studying the stationary state of radiation, in this paper we extend the quantum jump method of Refs. [8,9] in order to evaluate the reduced Green operator for the field. After calculating the Green operator, the stationary state is obtained as the eigenvector corresponding to unit eigenvalue. We will see that new features of the field arise for large mean number of atoms $\overline{N} \geq N_{\rm ex}$: in particular, a fine structure of thresholds is exhibited.

Before analyzing the Green operator Monte Carlo method, let us first describe the pump model considered here. Atoms from a monoenergetic beam are excited to the upper masing level by means of a periodically pulsed laser. Then they cross the micromaser cavity that is resonant with an atomic transition to a lower lying masing level; we suppose that the ground state atoms are far out of resonance, thus atoms not excited by the laser pulse do not affect the cavity field. Each laser pulse excites a cluster of atoms. The pulse is sufficiently short so that each cluster can be considered pointlike with respect to the cavity length. The number N of excited atoms per cluster is given by a Poisson distribution with average number $\overline{N}$. For a pulsing period T, the injection rate of excited atoms is $r = \overline{N}/T$. For fixed r, in the limit $\overline{N} \to 0$, $T \to 0$ one recovers the original one-atom Poisson-injected maser of Refs. [1,2]. We are interested in the stationary properties of the field, which in this context is considered at stroboscopic times $t_j = jT$ ($j = 0, 1, \ldots, \infty$), namely at the injection times of clusters in the cavity. We fix for simplicity $T = \tau_{\rm int}$, where $\tau_{\rm int}$ is the interaction time of each cluster in the resonator. The evolution of the joint radiation-atom density matrix R between two consecutive times t_j, t_{j+1} is described by the following master equation in the interaction picture:

$$\frac{dR}{dt} = \mathcal{L}_N R \equiv -\frac{i}{\hbar}[H_N, R] + \mathcal{L}_f R \,. \tag{1}$$

In Eq. (1) H_N is the Hamiltonian describing the interaction between radiation and a N-atom cluster—in the rotating wave approximation—namely

$$H_N = -i\hbar g a \sum_{j=1}^{N} \sigma_+^{(j)} + \text{H.c.} \,, \tag{2}$$

whereas $\mathcal{L}_f$ is the free field Liouvillian, such that

$$\mathcal{L}_f R = -\frac{\gamma}{2}(n_b + 1)(a^\dagger a R + R a^\dagger a - 2 a R a^\dagger) - \frac{\gamma}{2} n_b (a a^\dagger R + R a a^\dagger - 2 a^\dagger R a) \,. \tag{3}$$

In Eqs. (2) and (3) a and $a^\dagger$ are the annihilation and creation operators of the field mode, $\sigma_\pm^{(j)} = (\sigma_x^{(j)} \pm i\sigma_y^{(j)})/2$ are the Pauli matrices describing the two masing levels of the jth atom in the cluster, g is the atom-radiation coupling constant, γ^{-1} is the photon lifetime, and n_b is the number of thermal photons in the cavity (in the present paper we set $n_b = 0$).

When the cluster exits the cavity—immediately before that another one enters it—the radiation state is obtained upon tracing the joint density matrix R over atomic variables. We denote by ρ_j the radiation state at $t = t_j$, immediately before a N-atom cluster enters the cavity. At $t = t_{j+1}$ the field density matrix is

$$\rho_{j+1|N} = \mathrm{Tr}_a \left[\exp(\mathcal{L}_N \tau_{\rm int}) \rho_j \otimes |\uparrow\rangle_{N\,N}\langle\uparrow|\right] \equiv \mathcal{G}_{|N}\, \rho_j \,, \tag{4}$$

 0031-9007/95/74(6)/900(4)$06.00

where $|\uparrow\rangle_{N\,N}\langle\uparrow|$ denotes the state of the N-atom cluster entering the resonator with all atoms in the upper masing level. In Eq. (4) both the density matrix $\rho_{j+1|N}$ and the reduced Green operator of the field $\mathcal{G}_{|N}$ are *conditioned* by N. In this way, one describes the stroboscopic field dynamics for a particular sequence of clusters. We are interested in the field dynamics averaged on all possible sequences of clusters: this corresponds to consider unconditioned quantities, which are obtained upon averaging over the probability distribution of N, namely

$$\rho_{j+1} = \overline{\mathcal{G}_{|N}}\,\rho_j\ , \tag{5}$$

where $\overline{\mathcal{G}_{|N}} \equiv \sum_N p_N \mathcal{G}_{|N}$, and

$$p_N = \exp(-\overline{N})\frac{\overline{N}^N}{N!}\ . \tag{6}$$

After m clusters, with number of atoms $N_1, N_2, \ldots, N_m$, have crossed the cavity, the conditioned field state at $t = t_{j+m}$ is obtained multiplying ρ_j by the sequence of Green operators $\mathcal{G}_{|N_m}\cdots\mathcal{G}_{|N_2}\mathcal{G}_{|N_1}$. Since the cluster beam is Markovian—the number of atoms of the ith cluster is independent on that of the jth cluster—the average is factorized as follows:

$$\overline{\mathcal{G}_{|N_m}\cdots\mathcal{G}_{|N_2}\mathcal{G}_{|N_1}} = \overline{\mathcal{G}_{|N}}^m. \tag{7}$$

Hence, the average Green operator $\overline{\mathcal{G}_{|N}}$ describes the whole stroboscopic dynamics. In particular, the stationary field is given by the eigenvector of $\overline{\mathcal{G}_{|N}}$ corresponding to unit eigenvalue (which is not degenerate). Because of the trace over atomic variables in Eq. (4), a diagonal field state ρ_j remains diagonal under the evolution and the (unique) stationary state is itself diagonal. Thus we restrict Eq. (5) to the number probability distribution $p_j(n) \equiv \langle n|\rho_j|n\rangle$. In matrix form we have

$$p_{j+1}(n) = \sum_{m=0}^{\infty} \overline{\mathbf{G}_{|N}(n,m)}\,p_j(m)\,, \tag{8}$$

where $\overline{\mathbf{G}_{|N}(n,m)}$ represents the average Green operator connecting diagonal states.

It is now easy to envisage a method for evaluating the matrix $\overline{\mathbf{G}_{|N}(n,m)}$ based on the quantum-jump Monte Carlo technique of Refs. [8,9]. With this method, the evolution of R in Eq. (1) is simulated through an ensemble average over many trajectories, that start from pure states $|m\rangle\langle m| \otimes |\uparrow\rangle_{N\,N}\langle\uparrow|$. Quantum jumps occur randomly on each trajectory, simulating the nonunitary evolution due to the lossy term $\mathcal{L}_f R$. For a fixed N-atom cluster, the mth row of the conditioned matrix $\mathbf{G}_{|N}(n,m)$ is evaluated upon tracing the joint matrix $\exp(\mathcal{L}_N\tau_{\rm int})|m\rangle\langle m| \otimes |\uparrow\rangle_{N\,N}\langle\uparrow|$ on atomic variables. Then, $\mathbf{G}_{|N}(n,m)$ is obtained by ranging over m. Actually, N is a random number, and the matrix $\mathbf{G}_{|N}(n,m)$ averaged over N is directly obtained using a random N [distributed according to Eq. (6)] for each trajectory [10]. This procedure could be used also for averaging over other random parameters, like, for example, the cluster velocity. As a test of the present Green-function Monte Carlo method, the stationary photon distribution $p(n)$ has been simulated for the regularly injected one-atom maser, reproducing results from direct numerical evaluation of the Green function [11] within statistical errors of a few percent.

Now we present the results for the cluster micromaser. The system is completely specified by four parameters: γ, g, r, and $T \equiv \tau_{\rm int}$. Upon considering the photon lifetime γ^{-1} as the time unit, only three dimensionless parameters are left: g/γ, $\gamma\tau_{\rm int}$, and the mean number of excited atoms crossing the cavity during a photon lifetime $N_{\rm ex} \equiv r/\gamma$. Notice that in terms of these parameters the average number $\overline{N}$ of atoms per cluster is

$$\overline{N} = rT \equiv N_{\rm ex}\gamma\tau_{\rm int}\,. \tag{9}$$

In the one-atom maser at steady state a general scaling law for the mean photon number $\langle n\rangle$ and normalized fluctuations $\sigma = \sqrt{\langle\Delta n^2\rangle}/\langle n\rangle$ holds around the maximum of $\langle n\rangle$ (for sufficiently high $N_{\rm ex} \gg 1$ and small numbers of thermal photons $n_b \ll N_{\rm ex}$). In particular, the maximum of $\langle n\rangle$ occurs for a fixed value of the pumping parameter $\theta = g\tau_{\rm int}\sqrt{N_{\rm ex}} \simeq \pi/2$, where the values of $\langle n\rangle/N_{\rm ex}$ and σ are almost independent of all physical parameters and of atomic pump statistics. The Monte Carlo simulation shows that such scaling also holds for many atoms in the cavity, provided that $\overline{N} < N_{\rm ex}$. This can be seen in Fig. 1, where $\langle n\rangle/N_{\rm ex}$ and σ are plotted versus $\overline{N}$ (which is normalized to $N_{\rm ex}$) for $\theta = \pi/2$. (For fixed $N_{\rm ex}$ we vary $\overline{N}$ by increasing $\gamma\tau_{\rm int}$; correspondingly g/γ must decrease, in order to keep $g\tau_{\rm int}$ fixed.) One can notice that in the range $0 < \overline{N} < N_{\rm ex}$ the variation of $\langle n\rangle$ is less than 5%, whereas σ is almost constant, namely the scaling law still holds true.

Figure 1 also shows that for $\overline{N} \simeq N_{\rm ex}$ the normalized variance σ increases abruptly with $\overline{N}$, and correspondingly $\langle n\rangle$ decreases in a sizeable way. The sudden change of σ vs $\overline{N}$ signals a dramatic modification of the cavity

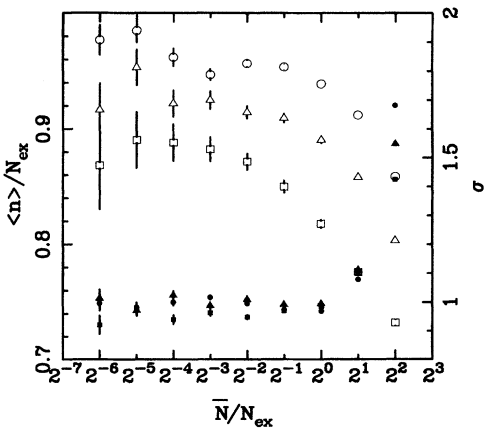

FIG. 1. Normalized mean photon number $\langle n\rangle/N_{\rm ex}$ (open symbols) and normalized variance σ (full symbols) at $\theta = \pi/2$ vs $\overline{N}/N_{\rm ex}$. [$N_{\rm ex} = 16$ (circles), $N_{\rm ex} = 8$ (triangles), $N_{\rm ex} = 4$ (squares). Error bars, when not visible, are contained in the plotted symbols.]

field as compared to the one-atom maser. To illustrate this point more generally, we consider the behavior of the mean photon number as function of the Rabi angle. In Fig. 2, $\langle n\rangle/N_{ex}$ is plotted versus $g\tau_{int}$, for $N_{ex} = 10$ and for different values of the parameter g/γ. Apart from the disappearance of trapping states, for $g/\gamma = 2.4$ the same quantitative behavior of the one-atom maser is found. This feature is almost unchanged for larger values of g/γ. On the contrary, for decreasing g/γ the behavior of $\langle n\rangle$ becomes very different, in the same fixed interval of $g\tau_{int}$. Indeed, $\langle n\rangle$ exhibits an increasing number of maxima, namely, a fine structure of the first threshold emerges (Fig. 1 monitors the small shift of the first peak). Correspondingly, the normalized variance σ exhibits an analogous splitting, as shown in Fig. 3. After considering the values of the mean number of atoms per cluster $\overline{N}$ in Figs. 2 and 3, one concludes that for $\overline{N} < N_{ex}$ the cluster micromaser behaves similarly to the one-atom maser, even for $\overline{N} > 1$; new features due to cluster injection become apparent only for $\overline{N} > N_{ex}$.

A more precise illustration of mechanisms underlying the fine structure of thresholds is given by analyzing the photon probability histograms at steady state, that

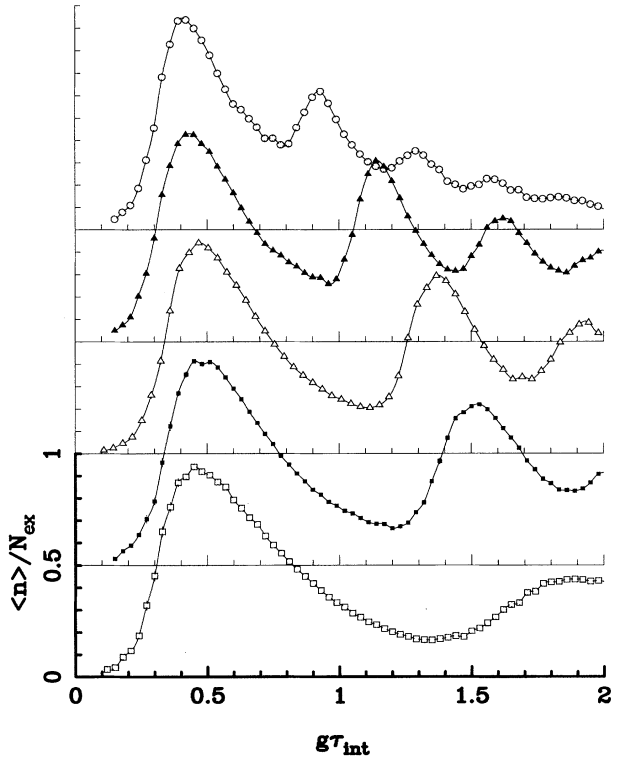

FIG. 2. Normalized mean photon number $\langle n\rangle/N_{ex}$ vs $g\tau_{int}$ for $N_{ex} = 10$. Curves corresponding to different values of g/γ are vertically shifted by 0.5. From the bottom to the top: $g/\gamma = 2.4, 0.96, 0.72, 0.48, 0.24$. At $g\tau_{int} = 0.497$ ($\theta = \pi/2$) the average numbers of atoms per cluster are $\overline{N} = 2.07, 5.17, 6.90, 10.35, 20.7$; at $g\tau_{int} = 2$, $\overline{N} = 8.33, 20.83, 27.78, 41.67, 83.33$. Error bars, when not visible, are contained in the plotted symbols.

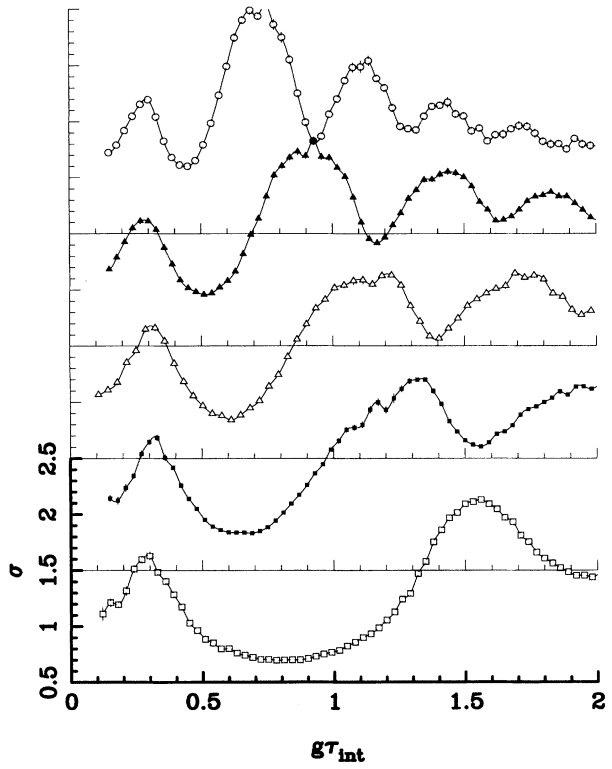

FIG. 3. Normalized photon fluctuations σ vs $g\tau_{int}$ for the same parameters in Fig. 2.

are given in Fig. 4 (for $N_{ex} = 10$ and $g/\gamma = 0.24$) at different values of the Rabi angles corresponding to local minima and maxima of $\langle n\rangle$. One can see that the photon distributions at minima are monotonically decreasing with n, resembling thermal probabilities (σ is slightly larger than the thermal value corresponding to the same mean photon number, and the peak at $n = 0$ is more pronounced). On the other hand, at the maxima of $\langle n\rangle$, $p(n)$ exhibits a peak for nonvanishing n, with a behavior more similar to a Poisson distribution (σ is slightly greater than unity). These general features of $p(n)$ near maxima and minima of $\langle n\rangle$ do not appreciably depend on the value of g/γ if $g/\gamma < 1$. For increasing g/γ the distribution around minima become less chaotic and more similar to the typical one-atom maser distributions. At maxima, the shapes of $p(n)$ slightly deviate from the Poisson in all cases. Notice that for all histograms the value of $p(n)$ at $n = 0$ is always exceptionally high, both for thermal- and Poisson-like distributions.

To illustrate the conditions leading to the fine structure of thresholds, we emphasize the physical meaning of all parameters involved in the present model. For fixed values of g/γ and N_{ex}, an increasing $g\tau_{int}$ corresponds to larger numbers of atoms $\overline{N}$. Physically this means that when slower atoms are selected, the laser pulsing period is simultaneously increased. On the other hand, decreasing g/γ with fixed $g\tau_{int}$ and N_{ex} corresponds to either one of the following setup modifications: (i) g and τ_{int} are

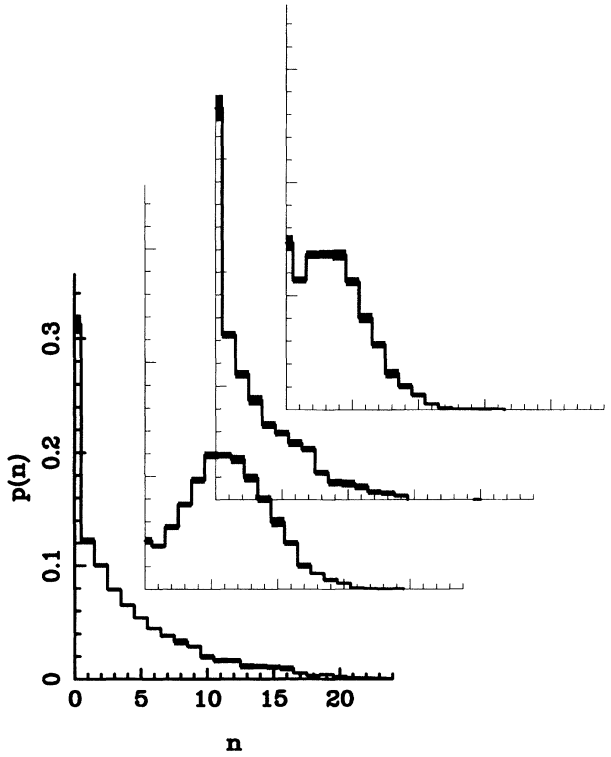

FIG. 4. Stationary photon probability distributions at $N_{ex} = 10$ and $g/\gamma = 0.24$ for different values of $g\tau_{int} = 0.78$, 0.93, 1.17, 1.29 (from the bottom to the top). For fixed g/γ, an increase of $g\tau_{int}$ corresponds to a rise of $\overline{N}$ [see Eq. (9)]: The corresponding average numbers of atoms $\overline{N}$ per cluster are $\overline{N} = 32.5$, 38.75, 48.75, 53.75. The mean photon numbers and normalized variances are $\langle n\rangle = 3.8 \pm 0.12$, 6.18 ± 0.07, 2.7 ± 0.1, 3.52 ± 0.06; $\sigma = 2.36 \pm 0.04$, 1.33 ± 0.02, 1.88 ± 0.03, 1.43 ± 0.02.

fixed, and the interaction takes place in a "worse" cavity (larger γ), with a higher injection rate to maintain the same $N_{ex} = r/\gamma$; (ii) τ_{int} is increased for fixed r, with a weaker coupling g to radiation in a cavity with the same photon lifetime γ^{-1}. In situation (i) the mean number of excited atoms per cluster $\overline{N}$ becomes larger due to the increase of r; in case (ii) $\overline{N}$ increases due to the increase of τ_{int}. Thus, the fine structure of the cluster-injected maser could be observed either with "large injection rate in a bad cavity," or with "weak coupling lasting for a long interaction time."

In conclusion, we presented the first numerical results on a many–atom micromaser at zero temperature, based on a Green-function Monte Carlo simulation. Clusters of N excited atoms (with N Poisson distributed) are periodically injected in the cavity. We focused attention on regimes with many atoms per cluster. The scaling law of the maximum radiation intensity and fluctuations still holds for more than one atom in the cavity. At $\theta = \pi/2$, deviations from the one-atom maserlike behavior are found for $\overline{N} \simeq N_{ex}$, where a transition occurs toward a novel cluster behavior. More generally, for any value of the pumping parameter θ, the transition from one-atom to cluster maser occurs when the average number of excited atoms per cluster exceeds the mean number of excited atoms entering the resonator in a photon lifetime. In this situation a fine structure emerges for the first threshold, with the appearance of multiple peaks for $\langle n\rangle$ and σ as functions of the Rabi angle. Even for zero temperature, at minima of $\langle n\rangle$ the stationary radiation tends to thermal-like distributions, as if the atomic beam in presence of losses played the role of a thermal bath [12]. At maxima of $\langle n\rangle$ the photon distribution is Poisson-like. This alternance of thermal and Poisson radiation, before and after thresholds—as in the customary laser—is a consequence of the competition between gain and loss mechanisms.

[1] D. Meschede, H. Walther, and G. Müller, Phys. Rev. Lett. **54**, 551 (1985).

[2] P. Filipowicz, J. Javanainen, and P. Meystre, Phys. Rev. A **34**, 3077 (1986); L. A. Lugiato, M. O. Scully, and H. Walther, Phys. Rev. A **36** 740, (1987); P. Meystre, G. Rempe, and H. Walther, Opt. Lett. **13**, 1078 (1988).

[3] Recent reviews on the micromaser can be found in H. Walther, Phys. Rep. **219**, 263 (1992); S. Haroche, in *Fundamental Systems in Quantum Optics,* edited by J. Dalibard, J. M. Raimond, and J. Zinn Justin (North-Holland, Amsterdam, 1992).

[4] The analytical solution of the microscopic master equation describing the one-atom maser in a very general context has been given in H.-J. Briegel, B.-G. Englert, C. Ginzel, and A. Schenzle, Phys. Rev. A **49**, 5019 (1994).

[5] E. Wehner, R. Seno, N. Sterpi, B.-G. Englert, and H. Walther, Opt. Commun. **110**, 655 (1994).

[6] M. Orszag, R. Ramírez, J. C. Retamal, and C. Saavedra, Phys. Rev. A **49**, 2933 (1994).

[7] R. Bonifacio, G. M. D'Ariano, R. Seno, and N. Sterpi, Phys. Rev. A **47**, R2464 (1993).

[8] R. Dum, P. Zoller, and H. Ritsch, Phys. Rev. A **45**, 4879 (1992).

[9] K. Mølmer, Y. Castin, and J. Dalibard, J. Opt. Soc. Am. B **10**, 524 (1993).

[10] All averaged quantities [the Green operator itself, but also the stationary distribution $p(n)$, etc.] are evaluated many times over different samples of trajectories, in order to obtain the statistical error bars of each quantity.

[11] G. M. D'Ariano, R. Seno, and N. Sterpi, J. Opt. Soc. Am. B (to be published).

[12] The nonzero probability of having $N > 1$ atoms in the cavity washes out the trapping states even for $\overline{N} < 1$ (see Refs. [5,6]). Thus, the results become less sensitive than in the one-atom maser to the thermal photon number n_b (for $n_b < \overline{N}$).